

Car Fires in Multi-Story Parking Garages

Serdar SELAMET¹
Burak AYVA²

ABSTRACT

Automated multi-story parking garages are modern alternatives to conventional parking structures to save space and volume in high demand parking spaces in urban areas. The design of such structures has significant knowledge gaps in terms of fire safety. The purpose of this study is to estimate the horizontal and vertical fire spread between passenger cars in automated multi-story parking garages and provide fire safety design to minimize fire spread and possible structural collapse. The fire spread between cars is established by estimating irradiance heat flux of each car component. An 8-floor automated multi-story parking garage with 56 passenger car capacity is designed in accordance with European standards. The results show that steel parking pallets underneath cars reach extreme temperatures about 1000 °C in early phases of fire for Category III vehicle fire with 8 MW maximum heat release rate, which could cause structural failure. Without any fire protection on the structure, the fire spreads to the car above in 23 minutes, to the neighboring car in 37 minutes and beyond the elevator shaft to the other cars in 82 minutes. The proposed sprinkler layout eliminates fire spread within 5 minutes. The most efficient way of passive fire protection is to seal steel pallet, its rail system and beams on the elevator shaft with 5 cm gypsum-based fire protection boards.

Keywords: Car fire, vehicle fire, parking garage, fire safety, fire resistance.

1. INTRODUCTION

The purpose of this study is to model and understand fire performance of an automated multi-story open parking garage including structural integrity, the energy content and heat release rate of passenger cars, horizontal and vertical fire spread and the effect of sprinkler locations. The goal is to provide additional active and passive fire safety measures in open car parks.

Fire safety design requirements for conventional open car parks are not strict. Automatic sprinkler systems, mechanical ventilation systems and passive fire protection on vertical

Note:

- This paper was received on August 30, 2022 and accepted for publication by the Editorial Board on March 3, 2023.
 - Discussions on this paper will be accepted by July 31, 2023.
- <https://doi.org/10.18400/tjce/1265492>

1 Bogazici University, Department of Civil Engineering, Istanbul, Türkiye
serdar.selamet@boun.edu.tr - <https://orcid.org/0000-0001-9444-470X>

2 Bogazici University, Department of Civil Engineering, Istanbul, Türkiye
burakayva@gmail.com - <https://orcid.org/0000-0002-7329-1019>

opening through floors are not part of NFPA 88A Standard [1]. According to NFPA 88A per Section 5.1.2, the height of an open car park is limited by 25 m for Type II (000) structures, whereas there is no limitation for Type I structures [1]. Such precautions may be valid for conventional open tall car parks; however, design of slabs and vertical openings are totally different in automated open tall car parks. Vertical opening area to total floor area is excessive in automated type car parks due to vertical lift openings. The vertical opening of lift system may act like an atrium rather than a simple vertical opening during a fire incident within an automated open tall car park; thereby changes vertical fire spread characteristics. Additionally, there is no slab fixed to the structural systems in automated open tall car parks. In such structures, car pallets docking and undocking between columns are utilized as carrying platforms of which structural fire response is unknown.

Passenger car fires in parking structures are not common, but such events can develop into large and uncontrollable fires [2]. Some cases of car park fires have involved hundreds of vehicles and caused structural collapses in the last two decades. A car park fire in Schiphol Airport in Amsterdam burned nearly 30 passenger cars and partly damaged around 101 passenger cars [3]. Another vital car park fire event is Kings Dock fire in Liverpool [4]. The fire led to a total loss of 1150 passenger cars. Firefighters have reported rapid lateral fire spread and vertical fire spread in both downward and upward directions. The most recent open car park fire has occurred in Stavanger, Norway [5]. With the effect of strong wind, flames engulfed the structure partially, a significant structural collapse has occurred, and around 300 passenger cars were destroyed. A few passenger car fire tests in full-size open car parks are carried out [6-9]. The general conclusion was that structural fire protection is not necessary for open deck car parking structures.



Fig. 1 - Automated multi-story parking garage with 4 units (Balıkesir, Turkey)

Automated multi-story parking garages are modern alternatives to conventional parking structures to save space and increase volume in high-demand parking regions in urban areas. They are generally constructed from steel. An 8-floor parking garage from Balikesir, Turkey, is shown in Fig. 1. It is an externally braced steel structure with embedded elevator and car pallets to store and retrieve passenger cars. These structures may be constructed with either open or closed façade.

Fire characteristics of passenger cars depend on vehicle size, ignition source and location, environmental conditions and ventilation level. Peak HRR levels vary within a wide spectrum, from 1.9 MW to 10.8 MW [2]. The high level of heat release rate per unit area during car fires increases the collapse risk of parking garages. Most of fire spread tests are based on lateral fire spread scenarios in the literature [10,11]. Weisenpacker et al. [11] focused on temperature levels around and inside of burning cars and did not measure the heat release rates (HRR). On the contrary, Park et al. [10] measured HRR by using large-scale calorimeter and the maximum HRR for the single-car fire was estimated as 3.5 MW. Studies suggest that HRR curves of passenger cars show no clear correlation with vehicle age [2].

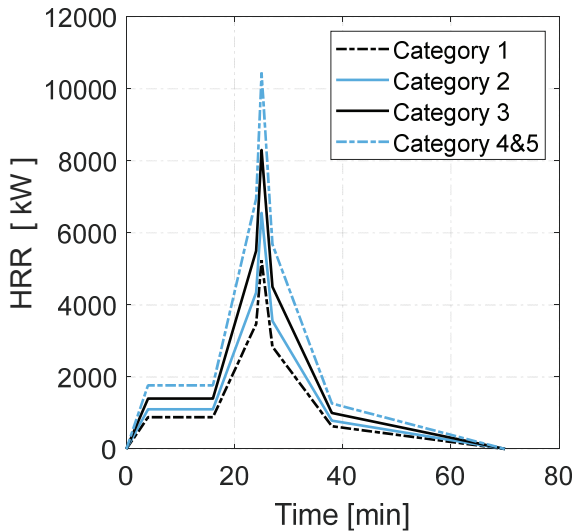



Fig. 2 - Equivalent HRR curves for classification of cars (adapted from Schleich et al. 1999 [12]).

The use of total combustion energy can classify passenger car fires during fire. The calorific potential classification that has five different categories is generally based on vehicle size and curb weight. Schleich et al. [12] have presented equivalent HRR curves for the potential calorific classifications of passenger cars in Fig. 2. The characteristics and trends of the HRR curves are identical. Schleich et al.'s [12] approach is based on the amplification of HRR values. In addition to the overall energy potential, ignition mechanism of individual components in vehicles are also essential to understand car fires. After the 1990s, the use of plastic components in passenger cars has increased from 5.1% in 1970s to 8.8% of car weight

in 2018 [2]. In addition to this, the average combustion energy per mass of plastic components within passenger cars has increased. Although the change in the mass of plastic materials is 72%, the total combustion energy has increased by 91% since the 1970s. The risk of fire spread from one car to another has risen with the increase in the use of plastic materials for exterior parts of passenger cars.

The occurrence of ignition can be forecast with a calculation of surface temperature if the substance is heated by convection and radiation. A set of test results of plastic vehicle components that used on outmost surfaces of passenger cars are given in Table 1 [13]. Ignition times under different irradiance levels and critical irradiance levels of plastic components are determined by tests [13]. All exterior plastic components excluding tires can be ignited by an irradiance level of 20 kW/m² in 7.5 minutes, whereas it takes less than 1 minute with an irradiance level of 30 kW/m². On the other hand, the ignition of tires takes much more time, but its critical irradiance level is not high.

Table 1 - Ignition times of plastic passenger car components [13] (NI: not ignited)



Component	Time to ignition (seconds) (NI=no ignition) Irradiance level				Critical irradiance level (kW/m ²)
	10 kW/m ²	20 kW/m ²	30 kW/m ²	40 kW/m ²	
Hub cap	NI	205	58	28	17.5
Mud flap	380	57	29	16	10
Wheel arch	NI	81	44	25	12
Bumper	NI	450	89	43	18.5
Bumper grill	NI	114	44	19	17.5
Bumper trim	415	83	30	16	11.5
Fuel tank	NI	354	114	59	16.5
	10 kW/m ²	12 kW/m ²	15 kW/m ²	20 kW/m ²	
Tire	NI	1100	597	240	11

Building Research Establishment (BRE) conducted a set of fire tests on fire spread modes between passenger cars [13]. All possible fire spread patterns between passenger cars are tested. These patterns are side-by-side fire spread, nose-to-nose fire spread and vertical fire spread at car stacker. Before and after photographs of tests are shown in Fig. 3. The gas temperature close to the ceiling has reached 1100 °C during side-by-side fire spread test. In the nose-to-nose fire spread test, the fire has spread to the next vehicle in approximately five minutes. In the case of car stackers, both cars in the stacker were engulfed in flames after 21 minutes.



Fig. 3 - Fire spread between passenger cars (BRE,2010 [13]).

One of the most critical knowledge gaps in suppression of passenger car fires is the effectivity of sprinkler systems in car stackers. Carpark fires are defined as ordinary hazard in most of national fire safety codes such as BS EN 12845:2015 [14], AS 2118:2017 [15], NZS 4541:2020[16] and the Turkish Regulation on Fire Protection [17]. BRE has conducted tests on the efficiency of sprinklers on passenger car fires for ordinary car parks and stacker systems [18]. The setup represents a closed car park, but ventilation is enough for a fuel-controlled fire. The fire started at the outermost passenger car. The first sprinkler was activated after 4 minutes, then all sprinklers were activated at the early stage of fire. The fire was not extinguished, and its thermal power reached around 7000 kW. However, the fire did not spread to the next vehicle. Cooling and transport effect of water droplets from sprinklers caused the smoke to drag down.

2. METHODOLOGY

In this study, an automated multi-story steel parking garage is designed based on an existing example shown in Fig. 1 and modelled in Fire Dynamics Simulator (FDS) [19] and SAP2000 [20]. A widely used design car fire HRR curve is modified to decrease computational demand of FDS and vertical and lateral fire spread criteria between passenger cars is defined via FDS simulations. Thermal response of structural members including the car pallets are obtained from FDS analyses.

2.1. Parking Garage

An 8-floor open-facade steel car park with 4 units and a capacity of 56 cars is designed according to Turkish Building Earthquake Code 2018 and Eurocode 3 [21,22]. Turkish Fire Regulation requires R15 rating for load-bearing structural elements for open parking structures with height 30.5 meters and below. Article 96c in the regulation mandates the use of sprinklers in garages, where more than 10 vehicles are taken into the garage through an elevator. However, the regulation does not specify sprinkler layout. The parking garage has a sprinkler system with a layout adopted by Australasian Fire and Emergency Service, which recommends placing the sprinklers on top of 4 vehicle corners. The reason behind this is merely an easy way of piping installation for sprinklers near four column-beam joints. Steel bracings are chosen as S235 grade. All remaining structural elements (i.e. beams and columns) are chosen as S275 grade. The structure is braced for lateral resistance. The structural system is designed in accordance to DD2 (10% - 50 year) design earthquake (TBDY 2018). The parameters used for the spectrum analysis are $S_S = 0.878$ s and $S_I = 0.214$ s with ZA soil condition, $R = 5$, $\Omega_o = 2$. All column cross sections are TUBO 160x160x10. The beams for the car pallet are HEA100 sections. The beams connecting to columns as part of the structural system are HEA140. The beams and columns are connected via shear connections. The structural design is shown in Fig. 4. Member cross sections are tabulated in Table 2.

Table 2 - Member sections of parking garage (see Fig. 4).

Member	Section
Columns	TUBO160x160x10
Beams	HEA140
Bracing	TUBO80x80x8
Car pallet beams	HEA100

Car pallets stay on wheels, which are mounted on short cantilever beams fixed to the columns. The car pallet is illustrated in Fig. 5. The pallet contains 4 longitudinal beams and 4 cross beams (HEA100) with a 2mm thick sheet metal above to carry the vehicle load. For the loading condition, the vehicle weight is taken as 2000 kg, which is an average weight of ordinary size SUV. Considering the vehicle as a live load (i.e. 1.6 live load factor), the vehicle load is applied as 4 point-loads of 7.85 kN on each pallet, which are 2.7 m apart from each

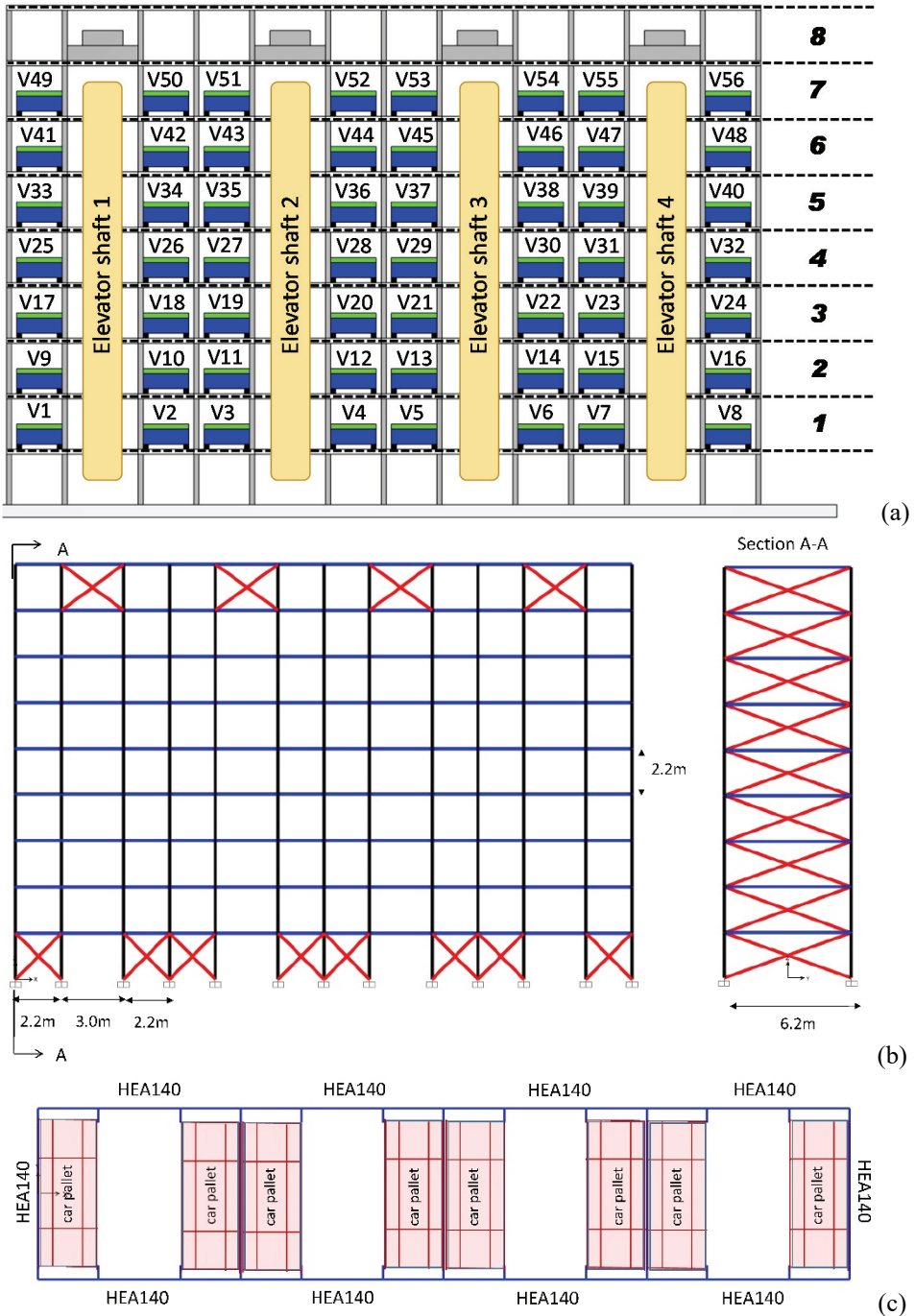


Fig. 4 - Multi-story parking garage: (a) illustration, structural design (b) elevation view and (c) top view.

other in accordance to the wheelbase of ordinary size SUV. Car pallet does not transfer moment or axial force to the cantilever beam supports. The elevator equipment on the top floor of each elevator shaft as seen in Fig. 4a is taken as 11 kN. The connection detail shown in Fig. 5 is commonly used in current parking garages and it does not transfer moment or axial force from the pallet to the main column.

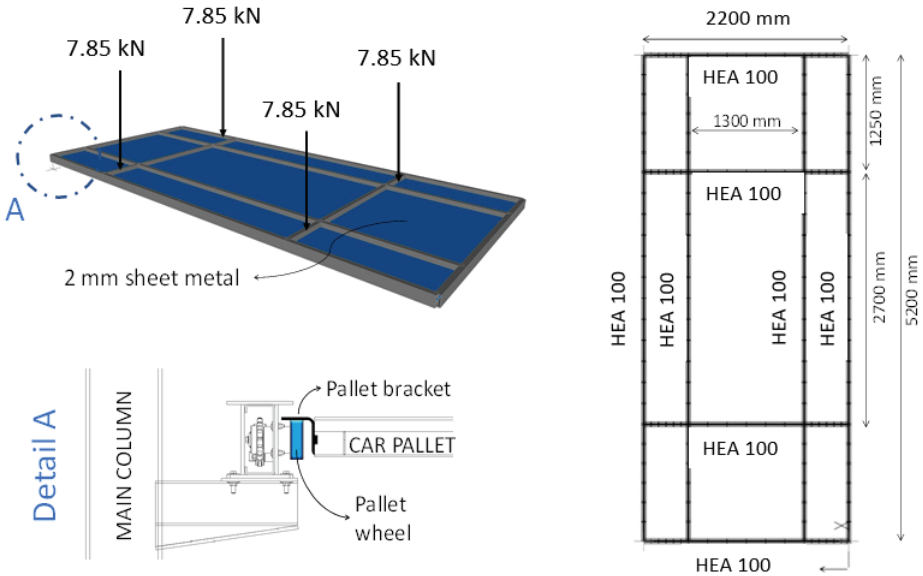


Fig. 5 - Car pallet design.

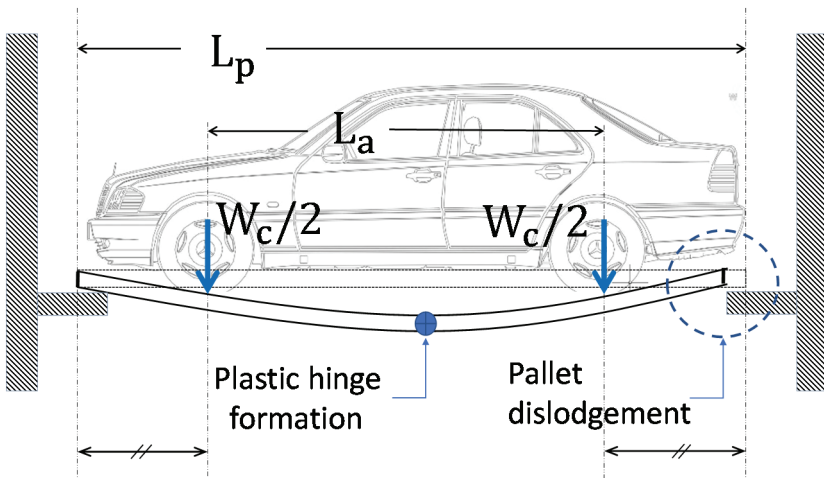


Fig. 6 - Car pallet collapse mechanism.

In this study, the thermo-mechanical analysis of the car park structural system is not conducted because both columns and beams under low utilization ratios μ have significantly high critical temperatures T_{cr} even without any fire protection. TUBO160x160x10 columns with $\mu = 0.129$ have $T_{cr} = 809$ °C. On the other hand, HEA100 beams underneath the car pallet carry a significant load and they are likely subjected to extreme temperatures from car fires just below. HEA100 beams with $\mu = 0.502$ have $T_{cr} = 590$ °C. A possible collapse mechanism of the car pallet is illustrated in Fig. 6 where a plastic hinge at the mid-span forms during fire. Such failure indicates that the pallet could collapse before the fire spreads to other cars.

2.2. FDS Model

The Fire Dynamics Simulator (FDS) model is created in PyroSim [23]. FDS solves numerically a form of Navier-Stokes equations appropriate for low-speed, thermally driven flow with an emphasis on smoke and heat transport from fires [19]. The turbulence is solved by Large-Eddy Simulation (LES). For the building model dimension and mesh size of this study, LES is the most suitable simulation type. For wildfires and large open space, very large eddy simulation is generally preferred. Direct numerical solver (DNS) is not suitable for this problem type.

The fire initiates from the car labeled as V13 on the 2nd floor as illustrated in Fig. 4a. No smoke control system is installed on the model. The heat and radiation transport calculation is performed with polyurethane as the fuel load and with 20 cm mesh size [24]. HEA100 and TUBO160x160x10 structural member surface temperatures are calculated utilizing the ‘exposed back condition’ in the FDS model, i.e. assuming that the members conduct heat through the cross-sectional thickness.

To estimate this cell size in the FDS model, the characteristic length scale of fire is calculated using Equation 1, where D^* is dimensionless diameter in m, Q is peak heat release rate (HRR) in kW, ρ_{∞} is ambient air density in kg/m³, T_{∞} is ambient temperature in °C, c_p heat capacity of air under constant pressure in J/kgK and g is gravitational acceleration in m/s².

$$D^* = \left(\frac{Q}{\rho_{\infty} T_{\infty} c_p \sqrt{g}} \right)^{2/5} \quad (1)$$

The heat release rate curve of Category III car is with a peak HRR of 8.3 MW, hence D^* is obtained as 2.235 m. It is suggested that for a reliable large eddy simulation (LES) at least 10 cells shall fit within the dimensionless diameter [25]. Therefore, 20 cm or smaller cell size with a simple chemistry model can be used. The cell size is chosen as 10 cm for all fire simulations in this study. Prandtl number, which relates the viscosity to the thermal conductivity is taken as 0.7 as recommended by FDS Technical Reference Guide [19] in case liquid droplets are simulated as water droplets from sprinklers. Radiative fraction is the fraction of energy released from the fire as thermal radiation. This number is set to 0.35. In FDS, the radiative fraction is defined between 0.3 and 0.4 for most combustibles and Table 16.1 in FDS Technical Reference Guide [19] takes 0.35 as default for all fuels other than liquid fuels such methane.

2.3. Passenger Car Design Fire

To reduce computational effort and shorten the run time on FDS simulations, both the heat release rate (HRR) curve and the vehicle model detail are modified without compromising the accuracy. For the passenger car design fire, Category III HRR curve with a peak HRR of 8.3 MW for maximum of 70-minute fire duration is modified as seen in Fig. 7. Schleich et al. [12] grouped the cars in five categories mainly due to their size (i.e. volume) and weight. Category III vehicle type (SUV) is defined to indicate the worst-case scenario. The modification mainly focuses on the ascent and descent parts around the peak point of the curve. Equations of ascent (\dot{q}_{asc}) and descent (\dot{q}_{dec}) heat flux of the Modified Category III fire curve are given in Eq. 2 and Eq. 3 where t is time in minutes and q is heat release rate in kW.

$$\dot{q}_{asc} = 11.8 t^2 \quad 11 \leq t \leq 25 \quad (2)$$

$$\dot{q}_{dec} = \dot{q}_{asc}(25) * e^{-(t-25)/6} \quad 25 \leq t \leq 70 \quad (3)$$

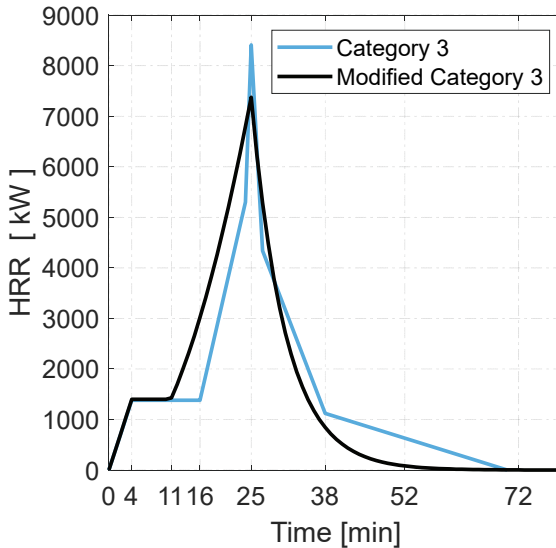


Fig. 7 - Category III design car fire [12] and Modified Category III fire.

As can be seen in Fig. 7, the cumulative thermal energy is shifted to the left in the Modified Category III fire with respect to the original curve. The decreasing phase is also faster so that the dying out of fire occurs quickly. This allows the flexibility to stop simulation earlier without compromising accuracy. The predefined termination of simulation is when the fire curve drops to 5% of its peak value at 43rd minute. The total energy release (i.e. area under HRR curve) is not violated by using the modified HRR curve. Differences between maximum gas temperatures are detected on a ceiling just above the fire pool as low as 50 °C, and maximum surface temperature levels are very similar in both cases [26]. High performance

computer used for the FDS analyses is 8-node Intel Xeon E5-2680 2.4 GHz with 128 Gb Ram per node. The case study FDS models consist of approximately 900,000 meshes and this modification in HRR curve results in 28% reduction of the computational time from 65 hours to 46 hours.

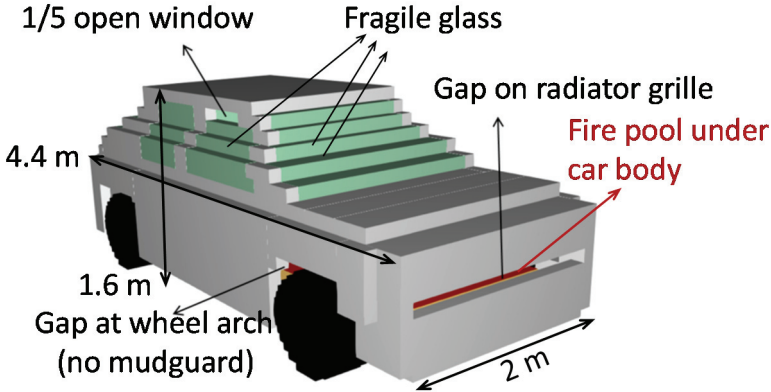


Fig. 8 - Car model in FDS.

A compact size car body encloses on a fire pool is designed in FDS with car body and window details as illustrated in Fig. 8. Metal parts in the body are defined as 1 mm steel sheet with 40 W/m.K of heat conduction coefficient. Windows are ordinary glass with 3 mm thickness and 1 W/m.K heat conduction coefficient. Glass breakage is simulated according to Weisenpacher et al. [11]. It is expected that windshield glass will break first followed by side and rear windows. The ground clearance of the passenger car is 20 cm.

2.4. Horizontal and Vertical Fire Spread Between Passenger Cars

‘NFPA-1710: Standard for the Organization and Deployment of Fire Suppression Operations, Emergency Medical Operations, and Special Operations to the Public’ by Career Fire Departments mandates 5:20 minutes response criterion for passenger car fires after the department is informed [27].

Joyeux [8] estimated the time duration needed for horizontal (lateral) fire spread between passenger cars as 12 minutes. In contrast, Li et al. [28] assessed the period as approximately 20 minutes, whereas Park et al. [10] reported the fire spread to an adjacent car at the 8th minute. Hence, the fire brigade must be alerted in a few minutes after the fire initiated.

Vertical fire spread between passenger cars is as important as lateral fire spread between passenger cars. However, the literature on this topic is very limited [13] [18]. To assess criteria for vertical fire spread; undercover, tires, and front bumper of the car given in Fig. 8 is modeled with combustible polymers. The undercover and bumper are chosen as polypropylene and the tires are selected as rubber. Thermal properties of materials used in the model are given in Table 3.

Table 3 - Thermal properties of materials in ignitable passenger car model

Material	Thermal Properties					
	Ignition Temp. [°C]	Specific Heat [kJ/kg.K]	Conductivity [W/m.K]	Heat of Combustion [kJ/kg]	Emissivity	Density [kg/m ³]
Rubber [29]	350	1.88	0.13	50	0.90	910
Polypropylene [29]	388	1.75	0.15	46	0.90	946
Steel [19]	-	0.46	45.8	-	0.95	7850
Glass [19]	-	0.79	1.0	-	0.05	2500

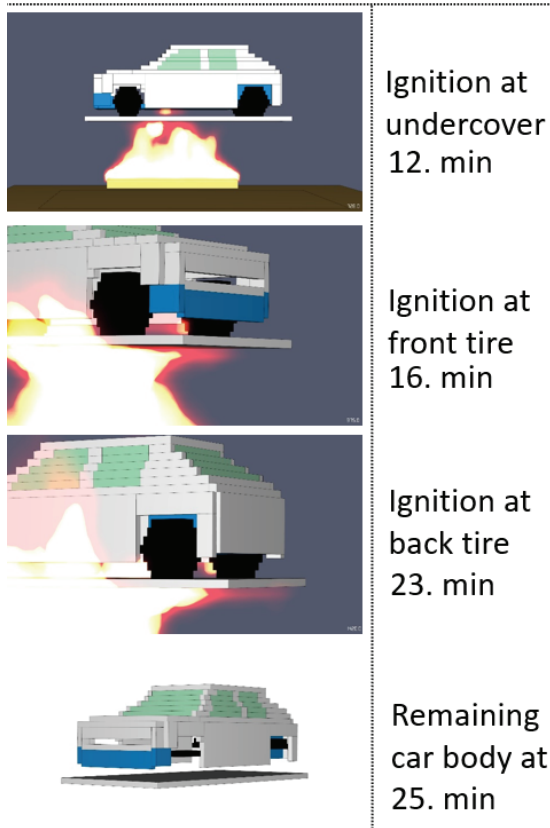


Fig. 9 - Vertical fire spread to a passenger car.

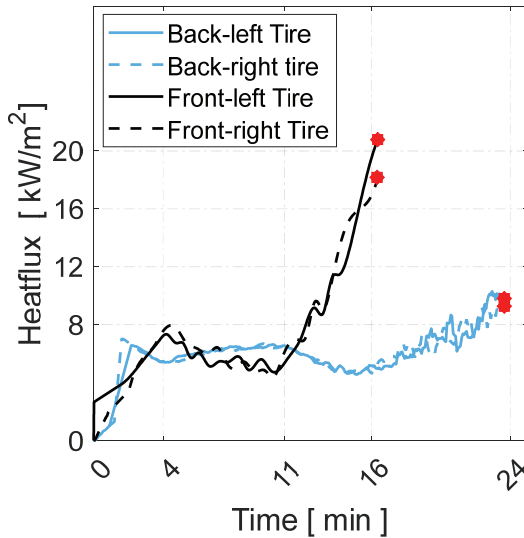


Fig. 10 - Incident surface heat flux on car tires (* : ignition time).

During the fire simulation, the first ignition occurred at the undercover of car, which is also observed in BRE tests [13]. The undercover in the simulation caught fire at $t = 12$ minutes. In BRE tests, the car above caught fire on the 5th minute and it was fully engulfed by $t = 10$ minutes where the peak HRR was measured as 8.5 MW on the 12th minute. BRE tests investigated the fire spread between cars directly stacked on top of each other without the steel pallet acting as a heat shield. The cars in the parking garage in this simulation are on different floors with 40 cm clear vertical distance from each other and 5 mm steel pallet as a heat shield. Hence, the fire spread times differ significantly. After the ignition of undercover, front tires ignite at 16th minute. The vertical fire spread is illustrated chronologically in Fig. 9. The result indicates that at approximately 10 kW/m^2 of incident surface heat flux is sufficient to start combustion on undercover. Incident surface heat flux curves for tires are shown in Fig. 10. The incident surface heat flux at ignition time nearly reaches to 20 kW/m^2 on front tires and 10 kW/m^2 on back tires.

With the aforementioned analysis, both vertical and lateral fire spread criteria are proposed. When the incident heat flux level is lower than 8 kW/m^2 , there is no risk of ignition, whereas the level is higher than 16 kW/m^2 , passenger cars start to burn and spread the fire. If the incident heat flux level is between 8 and 16 kW/m^2 , the adiabatic surface temperature [30] should be observed closely. As long as the adiabatic surface temperature is lower than the ignition temperature of the material, the related component cannot catch fire.

3. CASE STUDIES

In order to provide fire safety to automated multi-story parking garages, it is imperative to eliminate or slow down the fire spread between passenger cars. In addition, the structural

integrity including the steel pallets should be maintained during fire. Fire spread risk levels are shown in Fig. 11. Fire starts at vehicle V13 as shown in Fig. 4a. The neighboring passenger cars are designated as ‘R’ (right side of the car), ‘L’ (left side of the car), and ‘U’ (upper side of the car).

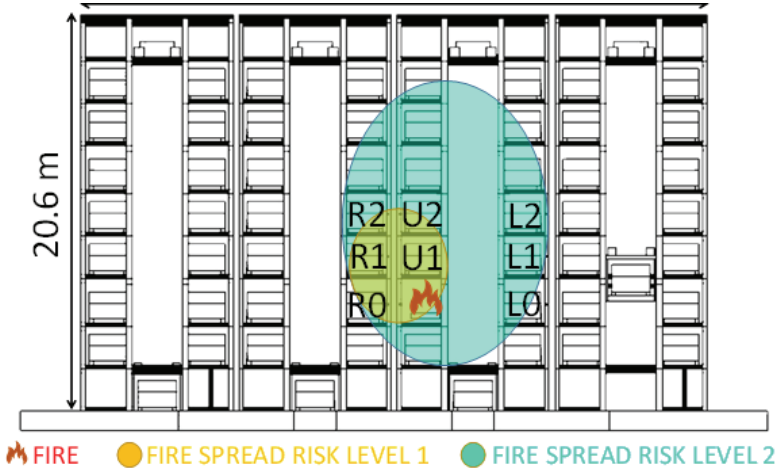


Fig. 11 - Automated tall car park: Fire origin at vehicle V13.

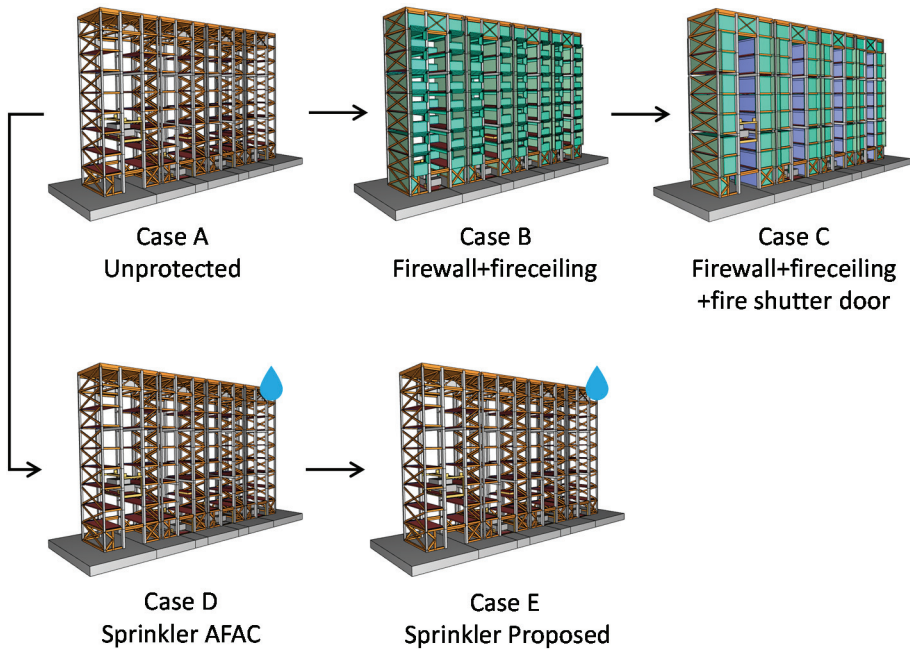


Fig. 12 - Case studies.

Case studies are illustrated in Fig. 12 with passive and active fire safety measures. In all case studies, Modified Category III HRR design curve is utilized. Unprotected car park is the base scenario without sprinklers (Case A). This study is conducted to understand the fire spread risks without any active and passive fire protection. The parking structure with partial firewalls and fireproof ceilings is shown in Case B. The structure with fire shutter doors is shown in Case C. Both Case B and C provide possible fire protection only. Finally, Case D utilizes the current (mandated) sprinkler active fire protection system in the parking garage and the sprinkler layout is adopted by [31]. Case E utilizes an improved sprinkler layout proposal.

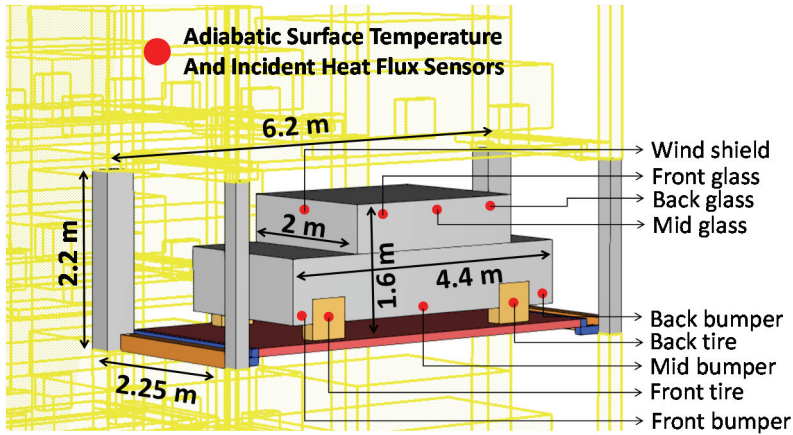


Fig. 13 - Sensor positions on passenger cars.



Fig. 14 - Nomenclature of structural elements around the fire zone

The passenger car model in Fig. 8 is used in FDS simulations. Adiabatic surface temperature and incident heat flux sensors shown in Fig. 13 are used as indicators for fire spread. The nomenclature of structural elements around the fire zone V13 over the car pallet P2E is shown in Fig. 14.

3.1. Case A: Car Park without Fire Protection

The fire safety level of an open façade unprotected car park is examined. Fig. 15 shows the development of vehicle fire in the car park. After 15th minute, hot gases and flames start to pervade the entire parking slot and upper areas. The gas temperature reaches to 900 °C under the upper car pallet P3E. It causes the ignition on the undercover of car U1 at 20th minute. Hot gases with 600°C are dragged up with buoyancy force and reach car U2 and R2. At 25th minute, the hot gas temperatures around the neighboring vehicle U1 and R1 reached 1100 °C as illustrated in Fig. 15. Passenger cars L0, L1 and L2 are at a relatively far distance from the fire, where the gas temperature remains low. Incident heat flux levels over these cars are under 5 kW/m² which is deemed safe as previously stated. Incident heat flux levels for car U1, R0 and R1 are given in Fig. 16. Incident heat flux levels at mid bumpers of upper cars reach over 50 kW/m² that causes fire to spread. Fig. 16 also indicates that the fire can spread to all surrounding cars within 25 minutes.

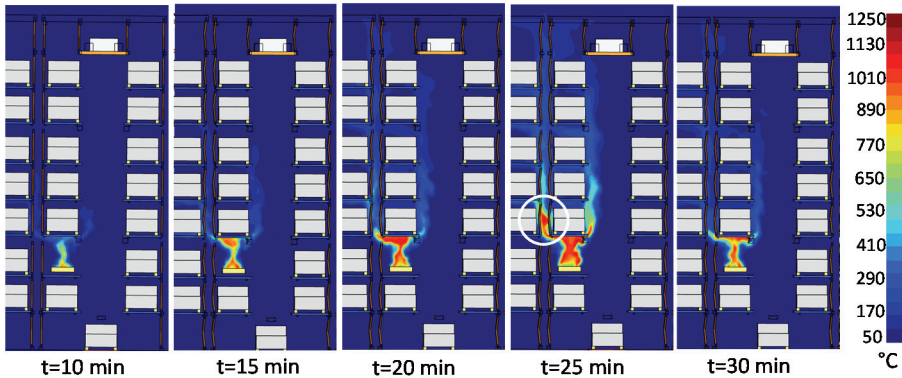


Fig. 15 - Gas temperature map (Case A)

The average temperatures of steel members are shown in Fig. 17. The average column temperatures (C2N1, C2N2, C3N1, C3N2) remain below 100 °C. The beam (B2E) near the elevator shaft (see Fig. 14) reaches as high as 800 °C, whereas the temperature level is much lower (i.e. 150 °C) in beams B2W and B3NE. This observation suggests that vehicle fire intensifies near the shaft where ventilation is expected to be at maximum levels. The beam underneath the car pallet P3E reaches temperatures as high as 1000 °C. It can be concluded that a possible dislodgement of the car pallet will occur at the early phase of fire because these beams have merely 590 °C critical temperature as calculated previously. Overall, the columns in the parking garage remain below critical temperatures and can be left without fire protection. The beams near the elevator shaft, however, go beyond the critical temperatures and exhibit a high risk of collapse and fire protection is necessary.

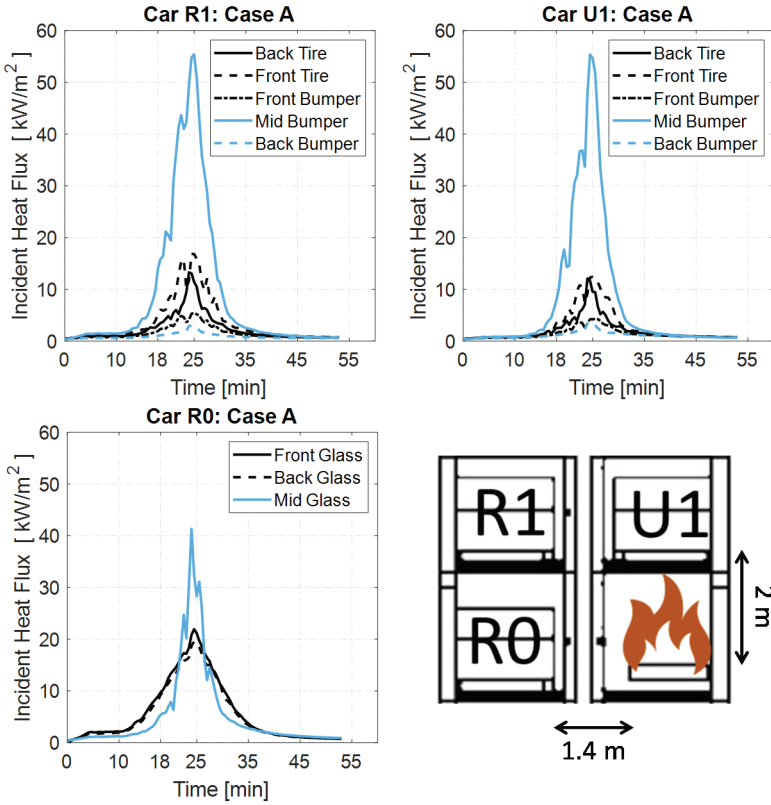


Fig. 16 - Incident heat flux levels on cars (Case A)

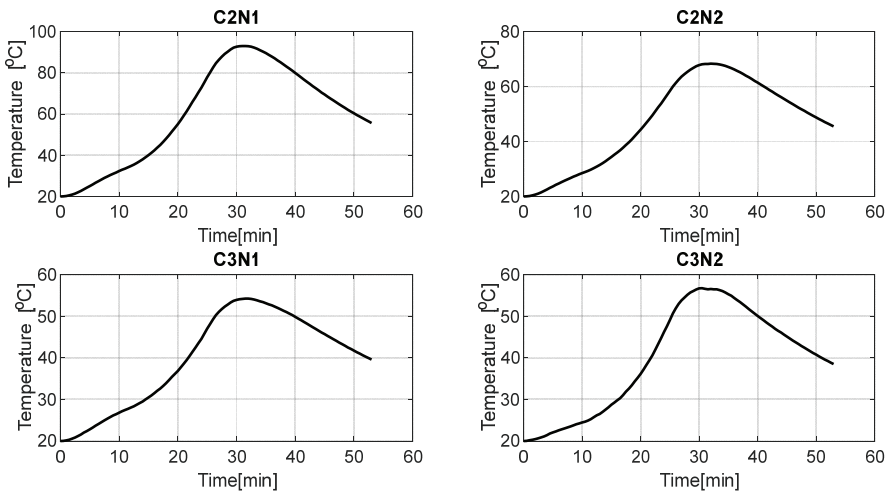


Fig. 17 - Average temperature levels of steel structural members (Case A). The steel pallet and beams near the elevator shafts reach critical temperatures.

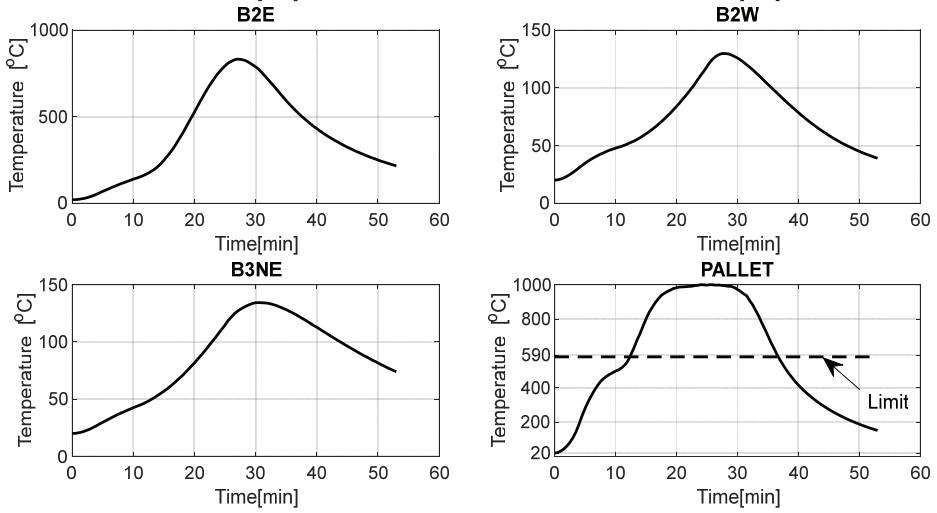


Fig. 17 - Average temperature levels of steel structural members (Case A). The steel pallet and beams near the elevator shafts reach critical temperatures. (continued)

3.2. Case B: Car Park with Firewalls

In order to minimize the fire spread, over 1800 m² of firewalls between passenger cars and outermost columns are placed throughout the structure. In addition, fire ceilings with 30 cm overhang are placed just underneath car pallets. The firewall configuration is seen in Fig. 18. By utilizing firewalls, hot gases are expected to channelize between the firewall and the overhang and exhausted through the façade. The firewalls are 5cm thick with 0.05 W/mK conductivity and 1 kJ/kgK specific heat. It is assumed that the thermal properties are temperature-independent and thereby stay constant throughout the fire.

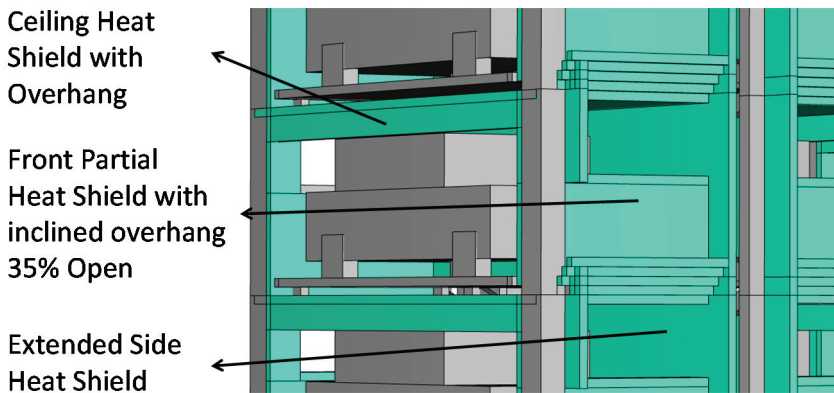


Fig. 18 - Fire wall configuration (Case B)

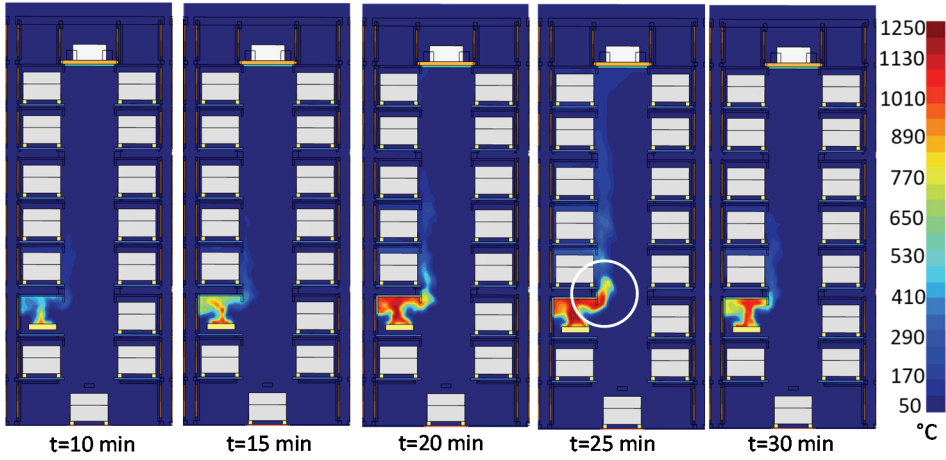


Fig. 19 - Gas temperature map (Case B)

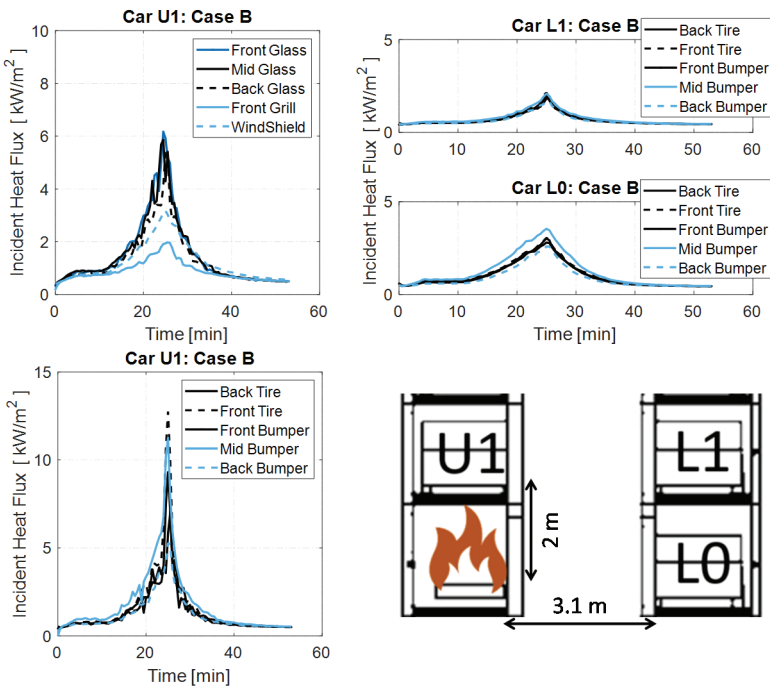


Fig. 20 - Incident heat flux levels on cars (Case B)

The gas temperatures in Case B show that the firewall and fire ceiling are mostly effective in preventing fire spread. The incident heat flux levels on neighboring passenger cars as given

in Fig. 20 are considerably lower compared to Case A. Car R0 and R1 are also totally protected by extended side heat shield as illustrated in Fig. 18. The vehicles on the opposite of the elevator shaft (i.e. L0, L1) are subjected to incident heat flux below 3 kW/m^2 and therefore the fire spread is eliminated in these vehicles. The mid bumper and the front tires of car U1 are exposed to an incident heat flux between 8 kW/m^2 and 16 kW/m^2 . Ignition temperatures for bumpers and tires were previously defined as $388 \text{ }^\circ\text{C}$ and 350°C , respectively. As seen in Table 4, the temperature levels obtained from the fire simulation are 382°C for mid bumper and 392°C for the front tire at 25th minute. Thus, the car U1 is assumed to catch fire at front tires. Case B significantly minimizes the fire spread but it cannot prevent it completely.

Table 4 - Maximum adiabatic surface temperatures of the car U1 at 25th minute

	Bumper			Tire	
	Front	Mid	Back	Front	Back
U1	348°C	382°C	252°C	392°C	293°C

3.3. Case C: Car Park with Firewalls and Shutter Doors

In Case C, fire shutter doors are placed between the slots and elevator shaft. In addition, all firewall overhangs are improved as seen in Fig. 21. A total of 2100 m^2 firewall is required for this design. This design approach aims to convert the fuel-controlled fire into the ventilation-controlled fire once the fire shutter doors are activated. The activation time or triggering mechanism of the fire shutter is essential. Fire shutters can be triggered not only electronically but also mechanically. If the triggering mechanism fails, and the electric motor is disabled, the fire shutter should be closed manually by security personnel or firefighters. The previous FDS results reveal that the activation time of 15 minutes to close the fire shutter is deemed to be satisfactory.

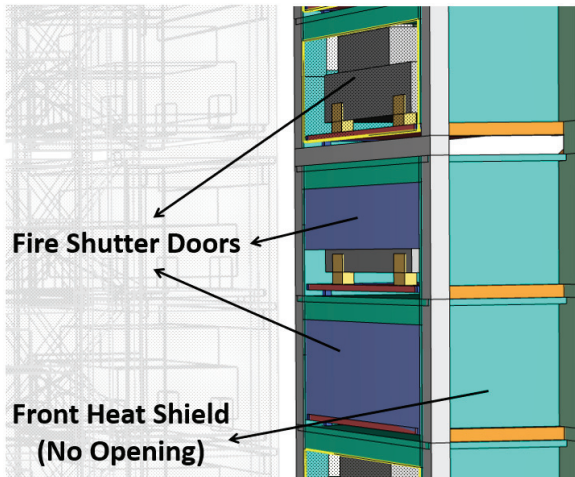


Fig. 21 - Improved fire wall configuration with fire shutter doors.

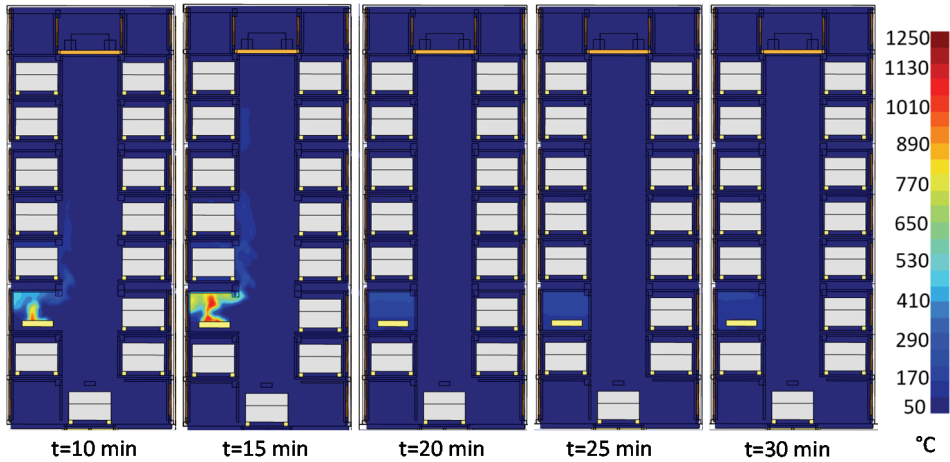


Fig. 22 - Gas temperature map (Case C)

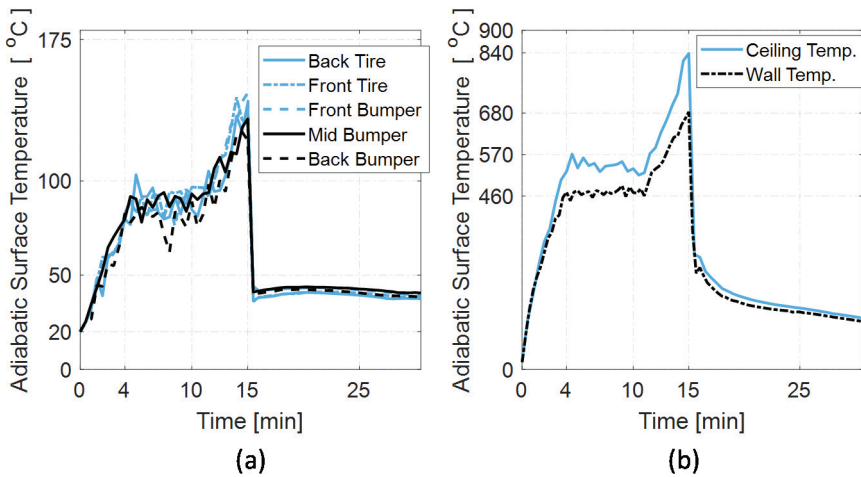


Fig. 23 - Temperature levels: (a) car UI, (b) shutter door and ceiling.

As seen in the gas temperature map Fig. 22, hot gases rising to car U1 are not able to cause an ignition before 15th minute, i.e. before the fire shutter doors are shut. After the fire shutter door is activated, the combustion reaction rapidly consumes oxygen in the compartment and the fire burns out. The maximum adiabatic surface temperature on car U1 is lower than 175 °C as seen in Fig. 23a. This level of adiabatic surface temperature does not cause ignition of any car component. Incident heat flux levels on all neighboring cars are also under 3 kW/m² as can be seen in Fig. 24. Temperature levels near the burning car reach to 850 °C, and the fire duration is limited to 30 minutes as seen in Fig. 23b. In conclusion, Case C has adequate fire safety with the combination of fire shutter doors and firewalls. However, the cost of such level of fire protection outweighs the benefit of complete elimination of the fire spread.

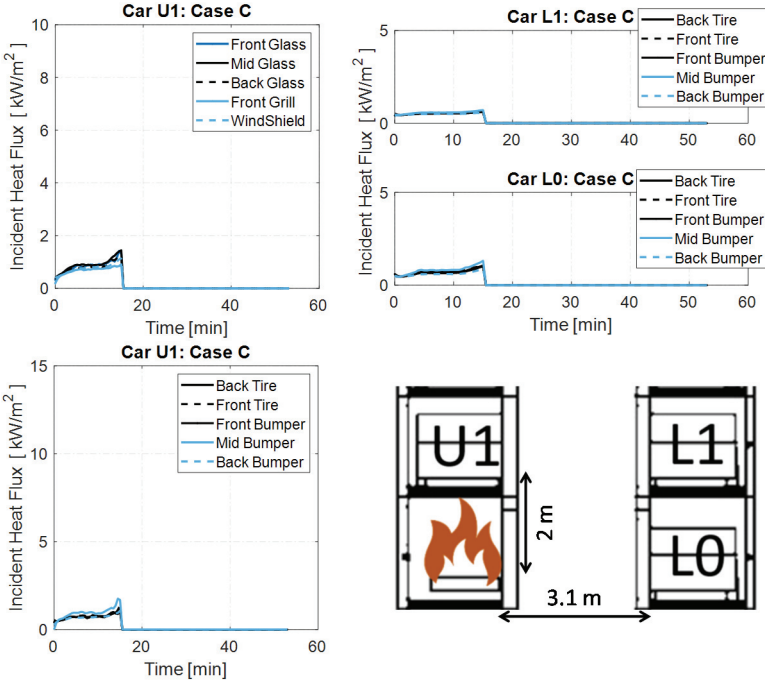


Fig. 24 - Incident heat flux levels for cars (Case C, fire shutter doors are closed after 15 minutes).

3.4. Case D and Case E: Car Park with Sprinklers

The main purpose of sprinkler water on a fire zone is to create a cooling effect by absorbing heat during phase change from liquid to vapor [32]. FDS is capable of modelling heating up and evaporation of water droplets engulfed by hot gases or over a hot surface. FDS is also adequate to model a reduction in HRR, while water droplets encounter the burning surface with predefined HRR curve. The main equation that governs the phenomena is given in Eq. 4 [19]. $\dot{q}_o''(t)$ is the predefined heat release rate per unit area in kW/m². The term may be obtained by dividing time dependent HRR to the area of the burning surface. The term k is calculated by Eq. 5, in where m_w'' is the local mass of water per unit area in kg/m², a is an empirical constant in m²/kg.s. The empirical constant is dependent on the water flux, material properties and global geometric features of the burning substance. Thus, it is strictly case-specific, and there is no study found that defines a coefficient for passenger car fires.

$$\dot{q}''(t) = \dot{q}_o''(t) e^{-\int k(t)dt} \quad (4)$$

$$k(t) = a m_w'' \quad (5)$$

The coefficient a is taken as 0.001 m²/kg.s. Same sprinkler nozzle is used in all cases. K factor is chosen as 160 L/min/√atm. The activation temperature and operating pressure are

78 °C and 1 atm. Latitude angles of conical jet stream are defined as 60° and 75° in the sprinkler spray model in FDS. Jet stream velocity is chosen as 5 m/s. Two different sprinkler system layouts are examined. The layouts are given in Fig. 25. The first layout is marked as ‘Case D’, which is the current sprinkler application in car parks suggested by Australasian Fire and Emergency Service Authorities Council Limited [31]. It contains one sprinkler at corners of each passenger car. The second layout is proposed by [26], which contains four sprinklers per passenger car at corners.

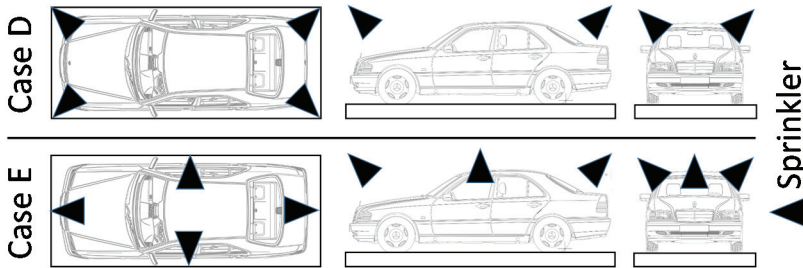


Fig. 25 - Sprinkler layouts: Case D proposed by AFAC [31] and Case E proposed by authors [26]

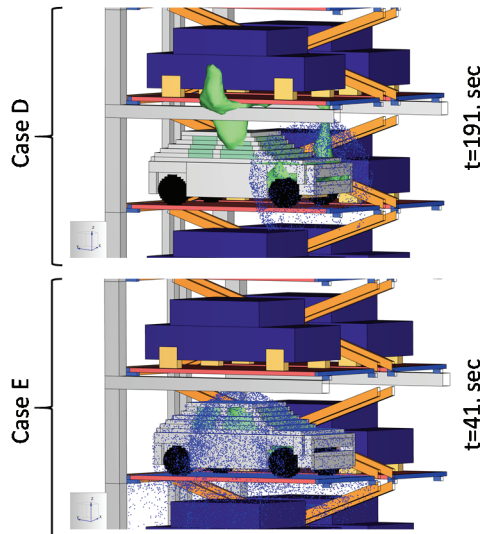


Fig. 26 - First sprinkler activation times.

Sprinkler activation is illustrated in Fig. 26. In the case D layout, the sprinkler at the south-west corner of the burning car is activated at 191st sec. Position of the sprinkler is not on the heat flow path from the gap on the front grill or the partially open window. It is the main reason for the relatively late sprinkler activation. In contrast, the sprinkler on the west of burning car is triggered at 41th sec. in the Case E because of its proper location. In the case, sprinkler water faces directly to the fire plume exhausted from side windows.

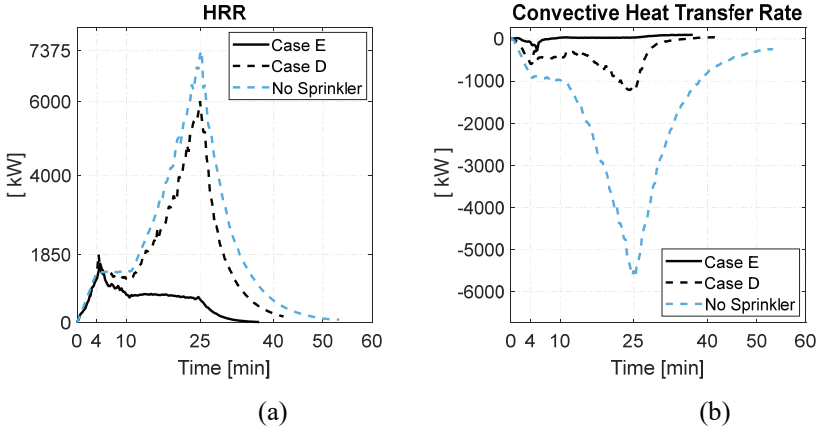


Fig. 27 - Effect of sprinklers: (a) on HRR, (b) on the convective heat transfer.

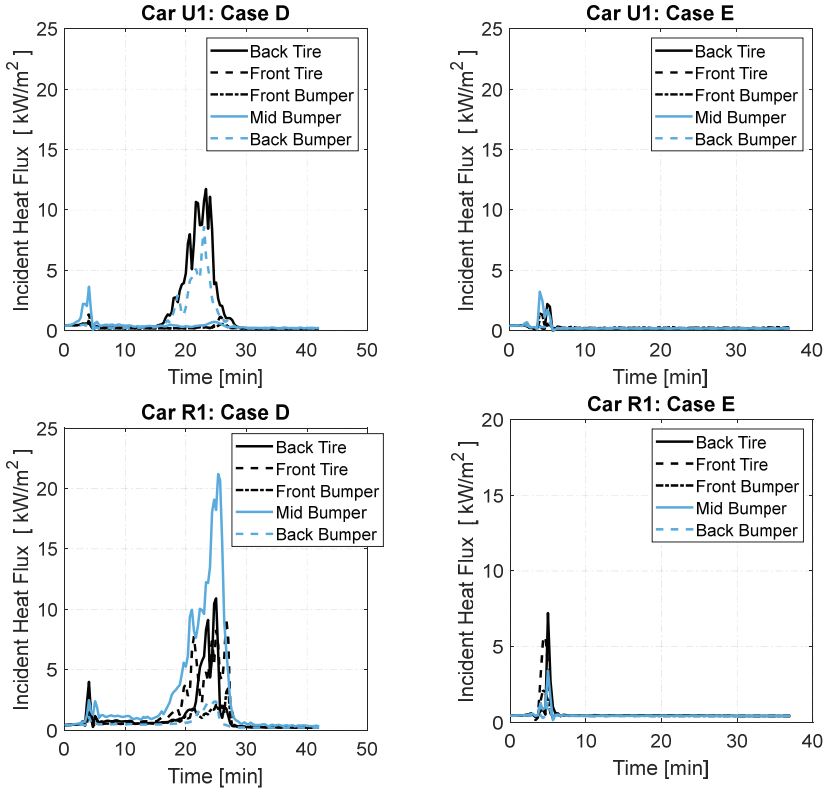


Fig. 28 - Incident heat flux on surrounding cars.

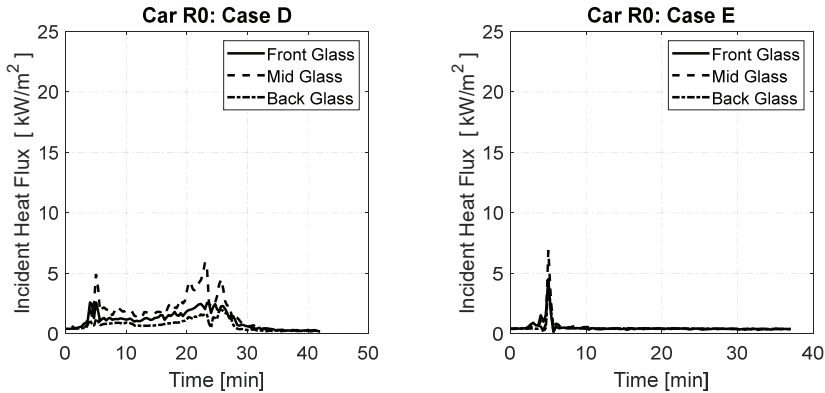


Fig. 28 - Incident heat flux on surrounding cars. (continued)

The reduction in HRR is directly related to the amount of water penetrating the fire surface. The sudden changes in HRR curves are shown in Fig. 27a. Sprinkler water also absorbs an important portion of total convective heat as shown in Fig. 27b. A similar phenomenon on convective heat transfer during a FDS simulation of a water mist spray on a propane burner has been observed in another study [32]. The incident heat flux levels on surrounding vehicles for both sprinkler layouts are shown in Fig. 28. The performance of the AFAC layout is satisfactory (Case D). Fire spread risk is eliminated for car U1 and R0 and, nearly 80% of convective heat is absorbed. However, the incident heat flux on the mid bumper of car R1 is still over 20 kW/m^2 . On the other hand, the proposed sprinkler layout in Case E not only prevents the fire spread but also suppresses it completely. Incident heat flux levels on all surrounding cars remain below 8 kW/m^2 .

4. CONCLUSIONS

In this study, the fire performance of an 8-story automated parking garage is investigated. The main goal is to find out the characteristics of vertical fire spread between passenger cars and add passive and active fire prevention measures to the structure to minimize the fire spread. Given the HRR of the passenger car, FDS model simulated the ignition times of nearby cars and realistically estimated the fire spread rate in multi-story parking garages. The study points out the most critical fire safety issues are (a) premature failure of steel car pallets and the rail system in automated parking garages, (b) fire spread risk to the cars above, adjacent and beyond the elevator shaft. Once the cars beyond the elevator shaft ignite at around 90 minutes, the structural system is considered as compromised.

These issues are addressed by firewalls and shutter door as passive fire safety measures. However, a complete fire spread elimination requires over 2000 m^2 firewall with combination of shutter doors, which is not cost effective. Instead, the priority is to keep the fire spread risk minimized as Risk Level 1 as illustrated in Fig. 11. Fire protection underneath the steel pallets and beams on the side of elevator shafts is required. The proposed sprinkler layout as active fire safety measure extinguishes the fire from the motor (i.e. front) and

broken glasses on the sides and back more efficiently and eliminates fire spread completely. Sprinklers need to function properly, which depends on the correct installation, continuous inspection of sprinklers, water supply and assumption of no power outage for pumps. This layout, however, requires additional piping installation along the beams.

The following conclusions are drawn:

- Without any passive and active fire protection on the parking garage, the fire spreads to the car above in 23 minutes, to the neighboring car in 37 minutes and beyond the elevator shaft to the other cars in 82 minutes.
- FDS simulations determined the ignition times and the order of ignition in the surrounding passenger cars. The ignition will start with undercover and tires and at incident heat flux levels higher than 16 kW/m². FDS simulations show that car components do not ignite if the incident heat flux levels are below 8 kW/m². These upper and lower bounds for heat flux for ignition are important findings in vehicle fire CFD investigations.
- NFPA-1710 mandates 5:20 minutes response criteria for passenger car fires. In order to prevent collapse of the parking pallet above the burning car, the fire brigade must be alerted within 7 minutes.
- During a car fire, all columns of the unprotected multi-story parking garage remain below their critical temperatures. Maximum column temperatures in all cases are under 200 °C. These temperature levels are not considered as significant to comprise the structural integrity. The beam temperatures on the façade remain below 150°C. The beams next to the elevator shaft reach critical temperatures as high as 800°C if left unprotected against fire.
- Steel car pallets are not robust against a passenger car fire. The member temperature of car pallet beams reaches to 1000°C at around 20th minute of fire. Plastic hinge mechanism will likely form in the load-bearing beams underneath the car pallet in the very early phase of fire. This means that a car pallet just above a fire may collapse before the fire spreads vertically to a car on the car pallet.
- The proposed sprinkler layout is efficient and eliminates the fire spread within 5 minutes. When the sprinkler heads are placed at the rear, front and sides of the cars as opposed to placing at the corners of the cars.
- Placing firewalls on the sides of the cars and adopting shutter doors to deprive the fire from oxygen are effective in preventing the fire spread but both architectural and cost concerns likely outweigh their performance.
- The most efficient way of passive fire protection is to seal steel pallet, its rail system and beams on the elevator shaft with 5 cm gypsum-based fire protection boards.

Acknowledgments

The authors acknowledge Newton Collaborative Research Programme NRCP1516/4/72, Bogazici University Scientific Research Project BAP: 13084D and 1002-TUBITAK Project: 218M550, which provided the funding for this study.

References

- [1] NFPA 88A Standard for Parking Structures 2019 Edition, Quincy, MA.
- [2] Boehmer and Klassen, CSE Combustion Science & Engineering: Modern Vehicle Hazards in Parking Garages and Vehicle Carriers, 2020.
- [3] L. Noordijk, T. Lemaire, Modelling of fire spread in car parks, *Heron*. 50 (2005) 209–218.
- [4] BAFSA British Automatic Fire Sprinkler Association, Kings Dock Car Park Fire. <https://www.bafsa.org.uk/wp-content/uploads/bsk-pdf-manager/2018/12/Merseyside-FRS-Car-Park-Report.pdf>, 2018 (accessed 27 June 2020).
- [5] FESG Fire Engineered Solutions Ghent, FESG provides explanation on Stavanger car park fire. <https://www.fesg.be/en/news/fesg-stavanger-car-park-fire>, 2020 (Accessed 27 June 2020).
- [6] I. D. Bennetts, D. Proe, R. Lewins and I. R. Thomas, Open-vehicle park fire analyses, Proceedings of the Pacific Structural Steel Conference, 1986, Auckland, New Zealand.
- [7] T. Kitano, O. Sugawa, H. Masuda, T. Ave and H. Uesugi, Large Scale Fire Tests of 4-Story Type Car Park Part 1: The Behavior of Structural Frame Exposed to the Fire at the Deepest Part of the First Floor, in Proceedings of the 4th Asia-Oceania Symposium on Fire Science and Technology, Tokyo Japan, 2000, pp. 527-538.
- [8] D. Joyeux, J. Kruppa, L.G. Cajot, J.B. Schleich, P. Van de Leur, L. Twilt, Demonstration of real fire tests in car parks and high buildings, Technical Steel Research Report, European Commission, Brussels, Belgium, 2002.
- [9] B. Zhao, J. Kruppa, Structural Behaviour of an Open Car Park Under Real Fire Scenarios, *Fire and Materials*, 28 (2004) 269-280.
- [10] Park, J. Ryu, H.S. Ryou, Experimental study on the fire-spreading characteristics and heat release rates of burning vehicles using a large-scale calorimeter, *Energies*. 12 (2019).
- [11] P. Weisenpacher, J. Glasa, L. Halada, Automobile interior fire and its spread to an adjacent vehicle, *J. Fire Sci.* 34 (2016) 305–322.
- [12] J.B. Schleich, L.G. Cajot, J.M. Franssen, J. Kruppa, D. Joyeux, L. Twilt, J. Van Oerle, G. Aurtenetxe. Development of design rules for steel structures subjected to natural fires in closed car parks, Technical Steel Research Report, European Commission, Brussels, Belgium, 1999.
- [13] BRE British Research Establishment, Fire Spread in Car Parks. BRE Report, Department for Communities and Local Government, London, UK, 2010.
- [14] British Standard Institution, BS EN 12845:2015 Fixed firefighting systems – Automatic sprinkler systems – Design, installation and maintenance.
- [15] Standards Australia, AS 2118.1:2017 Automatic fire sprinkler systems-General Systems.
- [16] Standards New Zealand, NZS 4541:2020 Automatic fire sprinkler systems.

- [17] Republic of Turkey Ministry of Environment and Urbanization, Binaların Yangından Korunması Hakkında Yönetmelik, Turkish Official Journal, 27344, (2009) 45.
- [18] BRE British Research Establishment, Sprinkler Protected Car Stacker Fire Test. BRE Technical Report, The British Automatic Fire Sprinkler Association, London, UK, 2009.
- [19] K. McGrattan, S. Hostikka, R. McDermott, J. Floyd, C. Weinschenk, K. Overholt, Sixth edition fire dynamics simulator technical reference guide volume 1 : mathematical model, NIST Spec. Publ. 1018. 1 (2015).
- [20] Computers and Structures Inc. SAP2000, Berkeley, California, USA, 2020.
- [21] Afet ve Acil Durum Yönetimi Başkanlığı, TBDY-2018 Türkiye Bina Deprem Yönetmeliği, Ankara, 2018.
- [22] EN 1993-1-2: Eurocode 3. Design of steel structures. Part 1–1: General rules – Structural Fire Design. European Committee for Standardization (CEN), Brussels, 2005.
- [23] Thunderhead, PyroSim 2020, Manhattan, Kansas, USA, 2020.
- [24] McGrattan K. B., McDermott R. J., Weinschenk C. G. and Forney G. P., Fire Dynamics Simulator User’s Guide. NIST special publication 1019.6, National Institute of Standard and Technology, Maryland, USA, 2013.
- [25] McGrattan K.B., Baum H.R., Rehm, R.G., Large eddy simulations of smoke movement, Fire Safety Journal 30:161–178, 1998.
- [26] B. Ayva, Performance-Based Fire Safety Design For Automated Vehicle Parking Steel Structures, Master’s Thesis, Bogazici University, 2020.
- [27] NFPA 1710 Standard for the Organization and Deployment of Fire Suppression Operations, Emergency Medical Operations, and Special Operations to the Public by Career Fire Departments 2020 Edition, Quincy, MA.
- [28] D. Li, G. Zhu, H. Zhu, Z. Yu, Y. Gao, X. Jiang, Flame spread and smoke temperature of full-scale fire test of car fire, Case Stud. Therm. Eng. 10 (2017) 315–324.
- [29] E.M. Pearce, Polymer Flammability. Am. Chem. Soc. Polym. Prepr. Div. Polym. Chem. 26 (1985) 198.
- [30] U. Wickström, A. Robbins, G. Baker, The use of adiabatic surface temperature to design structures for fire exposure, J. Struct. Fire Eng. 2 (2011) 21–28.
- [31] Australasian Fire and Emergency Service Authorities Council, Fire Safety Requirements for Automated Vehicle Parking Systems. AFAC Publication no 3044, East Melbourne, AU, 2020.
- [32] B. Merci, M. Shipp, Smoke and heat control for fires in large car parks: Lessons learnt from research?, Fire Saf. J. 57 (2013) 3–10. <https://doi.org/10.1016/j.firesaf.2012.05.001>.
- [33] S. Noda, B. Merci, F. Tanaka, T. Beji, Experimental and numerical study on the interaction of a water mist spray with a turbulent buoyant flame, Fire Saf. J. (2020) 103033.